Single-cell twitching chemotaxis in developing biofilms

Nuno M. Oliveira[a,b,1], Kevin R. Foster[a,b,2], and William M. Durham[a,2]

[a]Department of Zoology, University of Oxford, Oxford OX1 3PS, United Kingdom; and [b]Oxford Centre for Integrative Systems Biology, University of Oxford, Oxford OX1 3PS, United Kingdom

Edited by Howard C. Berg, Harvard University, Cambridge, MA, and approved April 19, 2016 (received for review January 15, 2016)

Bacteria form surface-attached communities, known as biofilms, which are central to bacterial biology and how they affect us. Although surface-attached bacteria often experience strong chemical gradients, it remains unclear whether single cells can effectively perform chemotaxis on surfaces. Here we use microfluidic chemical gradients and massively parallel automated tracking to study the behavior of the pathogen *Pseudomonas aeruginosa* during early biofilm development. We show that individual cells can efficiently move toward chemoattractants using pili-based "twitching" motility and the Chp chemosensory system. Moreover, we discovered the behavioral mechanism underlying this surface chemotaxis: Cells reverse direction more frequently when moving away from chemoattractant sources. These corrective maneuvers are triggered rapidly, typically before a wayward cell has ventured a fraction of a micron. Our work shows that single bacteria can direct their motion with submicron precision and reveals the hidden potential for chemotaxis within bacterial biofilms.

Pseudomonas aeruginosa | bacterial chemotaxis | twitching motility | Type IV pili | Pil-Chp system

Flagella-driven chemotaxis in bacteria has been thoroughly dissected (1–4), leading to its emergence as a paradigm of both signal transduction and cellular decision-making (4, 5). However, many key phenotypes of bacteria occur when cells are not swimming. In particular, planktonic cells commonly attach to surfaces and form communities, known as biofilms, which are central to health, disease, agriculture, industry, and the environment (6, 7). Biofilms often contain steep chemical gradients that result from cell metabolism, hampered diffusion, and the secretion of a wide variety of compounds (8). Although attached bacteria can be highly motile (9–11), remarkably little is known about the potential for these cells to respond to their chemical environment.

Surface-based movement has been studied in both *Myxococcus xanthus* (12, 13) and *Pseudomonas aeruginosa* (14–16) by exposing agar-based colonies to gradients of phospholipids and unsaturated long-chain fatty acids. Over time these colonies develop a bulge toward the chemoattractant source. However, the dense packing of cells within these assays makes it difficult to resolve the cause: asymmetric colonies can form because motility is simply enhanced on the side of the colony where chemoattractants are plentiful (chemokinesis), or instead because cells are actively biasing their motility up the chemical gradient (chemotaxis) (14). Moreover, in sharp contrast to swimming bacteria, experiments with *M. xanthus* have suggested that solitary surface-attached bacteria are incapable of biasing their motility along chemical gradients (13, 17). We, therefore, designed a new assay to test whether individual cells can perform chemotaxis on surfaces (*SI Appendix, SI Materials and Methods*). Our experiments reveal that not only are single cells capable of chemotaxis, but they can control their position with a striking level of precision.

Results and Discussion

Individual Bacteria Can Navigate Chemical Gradients on Surfaces. *P. aeruginosa* is an intensely studied opportunistic pathogen and a canonical model for the study of biofilms (18). After attaching to surfaces, *P. aeruginosa* cells are highly motile and move by pulling themselves along via the extension and retraction of their type IV pili, a process known as twitching motility (19). Although this form of movement is common throughout biofilm formation (10, 11), here we follow the movement of solitary bacteria in the early stages of biofilm development so that we can readily calculate each cell's chemical environment and resolve how it modifies their behavior. Importantly, the microfluidic assays used here are analogous to those used in classical studies of biofilm development (9–11), and the cells whose movement we analyze subsequently form 3D biofilm structures (Fig. 1 *F* and *G* and *SI Appendix*, Fig. S1). To generate stable chemical gradients, we use two inlet microfluidic devices where flow balances the smoothing effect of molecular diffusion (Fig. 1*A* and *SI Appendix*, Fig. S2 and *SI Materials and Methods*). Many bacterial chemoattractants strongly promote growth (20), which in our experiments leads to a crowded surface and a limited ability to analyze single cell behavior. We therefore began our experiments with DMSO, which is a known chemoeffector of bacteria (21–23) and, importantly, does not strongly affect growth in our experiments.

We used automated cell tracking to follow surface-attached *P. aeruginosa* cells that are exposed to a stable spatial gradient of DMSO (Fig. 1*A* and *SI Appendix*, Fig. S2). Our method allows us to follow large numbers of attached cells and quantify their individual responses to the presence, or absence, of a chemical gradient (*SI Appendix*, Fig. S3). In a DMSO gradient, we found that cell movement is strongly biased in the direction of increasing DMSO concentration (Fig. 1*B* and Movie S1), which contrasted with random motility in the absence of chemical gradients (Fig. 1 *C* and *D*). After 2 h of incubation, the chemotactic bias peaks, with more than three times as many cells moving toward the chemoattractant source than moving away from it ($\beta = 3.1$), but biased motility is maintained even as the surface becomes more crowded with cells (Fig. 1 *D* and *E*). These data show single cells direct their motility along chemical gradients and suggest that surface-attached cells are capable of chemotaxis [*sensu* Adler (1)].

Significance

Bacterial biofilms affect many aspects of our lives, from causing disease to promoting health and shaping many key processes in the environment. Despite this, surface-attached cells in biofilms are often portrayed as static and sluggish, a stark contrast to the energetic swimming they exhibit in liquid. Here we use microfluidic devices and automated cell tracking to challenge this view: We find that individual cells will actively move toward nutrients within a developing biofilm. This ability not only allows cells to seek out favored positions on a surface but our analyses show that they can regulate their movement with remarkable submicron precision. Our findings suggest we can systematically engineer biofilms by manipulating the movement of the cells from which they are founded.

Author contributions: N.M.O., K.R.F., and W.M.D. designed research; N.M.O. and W.M.D. performed research; N.M.O. and W.M.D. analyzed data; and N.M.O., K.R.F., and W.M.D. wrote the paper.

The authors declare no conflict of interest.

This article is a PNAS Direct Submission.

[1]Present address: Cell Biology Division, Medical Research Council Laboratory of Molecular Biology, Cambridge Biomedical Campus, Cambridge CB2 0QH, United Kingdom.

[2]To whom correspondence may be addressed. Email: kevin.foster@zoo.ox.ac.uk or william.durham@zoo.ox.ac.uk.

This article contains supporting information online at www.pnas.org/lookup/suppl/doi:10.1073/pnas.1600760113/-/DCSupplemental.

www.pnas.org/cgi/doi/10.1073/pnas.1600760113

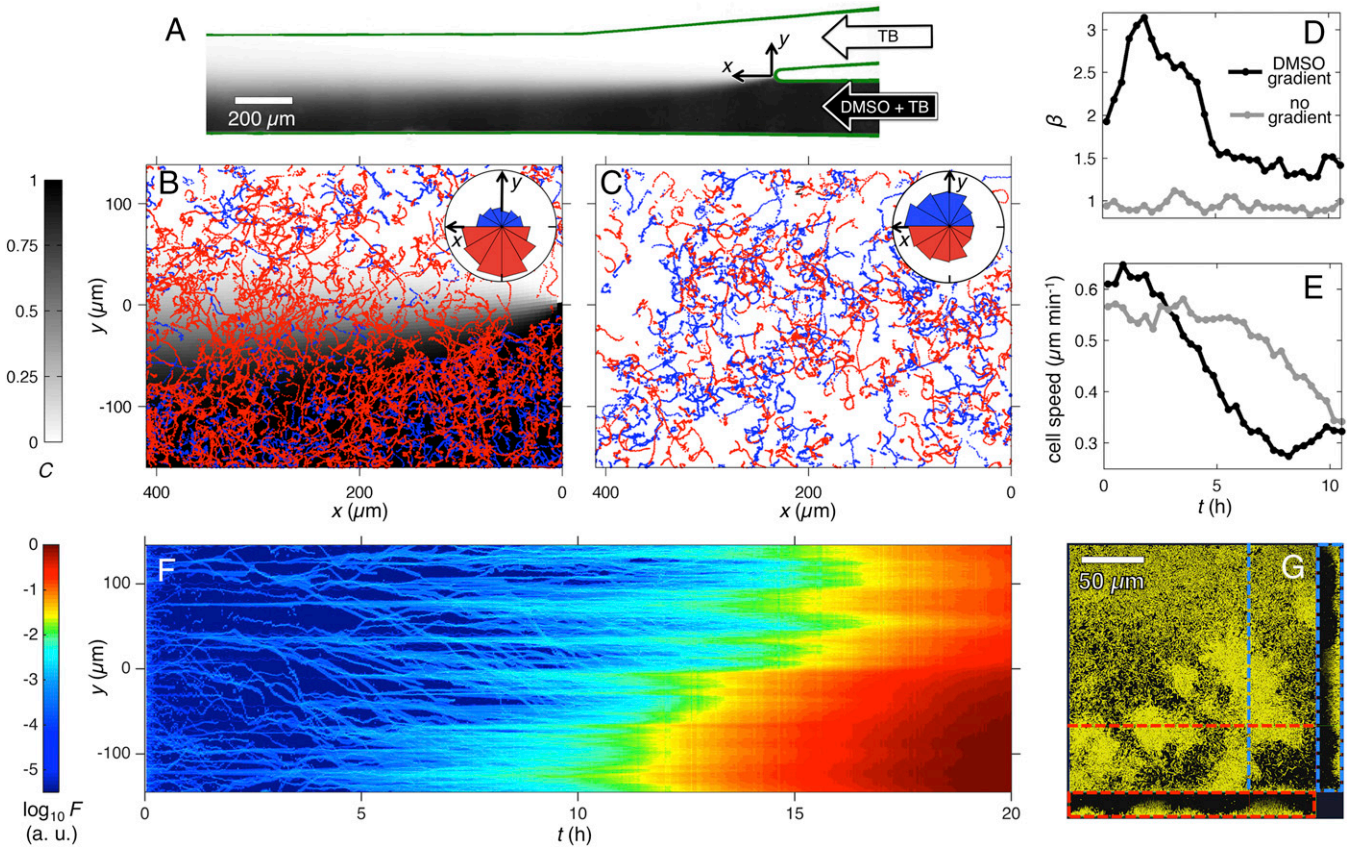

Fig. 1. Surface-attached *P. aeruginosa* cells direct their movement up gradients of DMSO during biofilm formation. (*A*) A two-inlet microfluidic device generates a stable chemical gradient via molecular diffusion. TB is continuously injected through one of the inlets, whereas DMSO at a concentration of C_{MAX} = 350 mM and TB are continuously injected through the other inlet. Here $C = C'/C_{MAX}$, where C' is the local concentration of DMSO that was quantified using fluorescein in a separate experiment (*SI Appendix*, Fig. S2 and *SI Materials and Methods*). (*B*) Cell trajectories over the first 5 h of the experiment (t = 0–5 h) show that motility is biased toward increasing concentrations of DMSO. Trajectories with net movement toward larger C (i.e., in $-y$) are shown in red and those with net movement toward smaller C (i.e., in $+y$) are shown in blue. The background shows C computed by a mathematical model (*SI Appendix*, Fig. S2). *Inset* shows probability density functions of the angle from each trajectory's origin to final position and red (blue) bins denote movement in the $-y$ ($+y$) direction (*SI Appendix, SI Materials and Methods*). This *Inset* also shows slight preferential movement in the $+x$ direction, which likely results from interactions with flow (39). (*C*) Control shows there is no bias in the y direction without DMSO. (*D* and *E*) A time series of the chemotactic bias, β, defined as the number of cells that move in $-y$ divided by the number moving in $+y$, peaks at $t \approx 2$ h (*D*; black line; gray line shows control) and then declines as the surface becomes more crowded and cell speed is attenuated (*E*). (*F*) A kymograph of the fluorescent intensity, F, of cells that constitutively produce yellow fluorescent protein (*SI Appendix, SI Materials and Methods*) show how biofilms develop over time in our experiments. Here we average the fluorescent intensity in x, allowing us to continuously resolve both the chemotaxis of cells (light blue streaks moving toward $-y$) and formation of densely packed biofilms (red). As biofilms produce a much brighter fluorescent signal than single cells we plot the logarithm of F so that both can be visualized. *SI Appendix*, Fig. S1 shows the raw images from which this kymograph was constructed. (*G*) A 3D confocal micrograph of the biofilm shown in *F*, imaged at t = 20 h, shows the biofilm is already many cells thick, extending ≈20 μm from the surface. Dashed lines indicate the positions of the vertical cross sections.

In our experiments, both cell division and motility cause cells to preferentially accumulate on the side of the device with the chemoattractant (Fig. 1*F* and Movie S1). To test whether the biased motility we observe is an artifact of the variation in cell density, which has been shown coordinate surface motility in *M. xanthus* (24), we exposed cells to a chemoattractant gradient that switched direction every 3 h. By minimizing crowding on one side of the channel, this assay also allows us to study the responses of individual cells to nutrients like succinate, which is a preferred carbon source of *P. aeruginosa* and a potent chemoattractant of cells in the planktonic state (25). When the chemoattractant gradient was inverted, cells responded by changing the direction of their bias to track the gradient (Fig. 2 *A*–*G*). The refinement with which individual cells dynamically track the gradient can be observed in Movie S2. Our data show then that cells are directly responding to the imposed gradient rather than to de novo gradients generated by the cells. Moreover, we observe these responses for gradients of both DMSO and succinate, the latter of which strongly stimulates both growth and cell motility (*SI Appendix*, Fig. S4). Finally, the increased data available from this second assay reveals that the chemotactic bias, β, increases with the magnitude of the chemoattractant gradient $|G|$ (Fig. 2*H*), which is a defining feature of chemotaxis across different biological systems (26). Based on the responses seen in our two single-cell assays (Figs. 1 and 2), we conclude that individual surface-attached bacteria are indeed capable of chemotaxis.

Attached *P. aeruginosa* Use Pili-Based Motility and the Chp Chemosensory System to Perform Chemotaxis. What is the genetic basis of the chemotactic response we documented above? After attachment, *P. aeruginosa* is well known to use pili-based motility to move on surfaces (9–11, 18, 19). Accordingly, a mutant that cannot generate functional pili (Δ*pilB*) is immobile in our experiments (Fig. 3 *A* and *C*), whereas a mutant that lacks flagella (Δ*flgK*) exhibits surface motility (*SI Appendix*, Fig. S5). We find flagella mutant cells stand upright and show increased motility relative to WT, which is in agreement with a previous study (27), and suggests that flagella may function as a stabilizing anchor during twitching motility. To explore if the flagella could play a role in chemotaxis, we studied the behavior of mutant that has a flagellum but lacks the ability to perform flagella-based chemotaxis. Chemotaxis in swimming

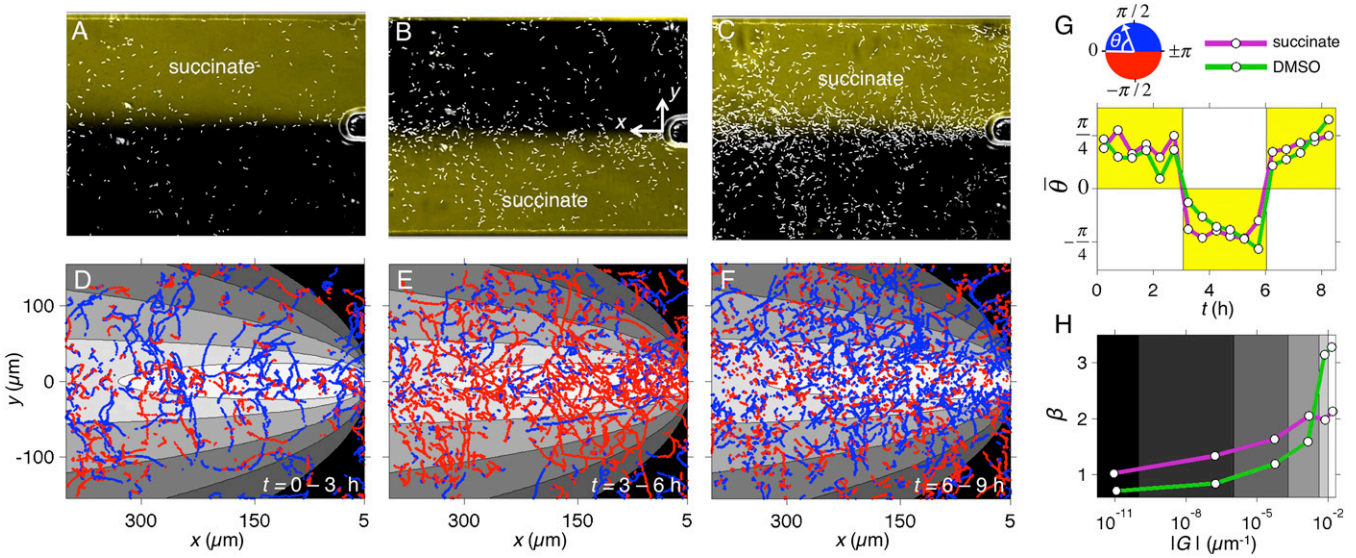

Fig. 2. Changing the direction of the chemoattractant gradient elicits a change in the direction of cell motility and reveals the chemotactic response increases with the strength of the gradient. (*A–C*) Cells (white spots) were exposed to gradient of succinate (visualized in yellow, C_{MAX} = 2 mM) whose direction was inverted every 3 h. (*D–F*) The resulting chemotactic response was measured by calculating the direction of cell movement, θ, over 16-min intervals, and segments of trajectories that moved in the $-y$ ($+y$) direction are shown in red (blue). (*G*) The mean movement direction, $\overline{\theta}$, was obtained by averaging θ for all cells (magenta line), revealing that cell motility is maintained in the direction of the instantaneous chemoattractant gradient (yellow regions). (*H*) Combining data from the entire experiment (t = 0–9 h) reveals that the chemotactic bias, β, increases with the magnitude of the normalized gradient, $|G| = 1/C_{MAX}\,|\partial C/\partial y|$ (magenta line). Here β is the number of trajectories moving in the direction of increasing concentration C, divided by the number moving in the direction of decreasing C. Grayscale colors in *D–F* show $|G|$ and correspond to the bins used in the analysis presented in *H*. Green lines in *G* and *H* show results of an analogous experiment conducted with a DMSO gradient (C_{MAX} = 350 mM). In both experiments, the position of chemoattractant was visualized using a dye that does not induce a chemotactic response (*SI Appendix*, Fig. S15), and $|G|$ was estimated using a mathematical model of diffusion (*SI Appendix, SI Materials and Methods*).

P. aeruginosa cells is under the regulation of a Che transduction system homologous to that of *Escherichia coli* (16, 28), and mutants in CheY1, the key response regulator, can swim but cannot actively bias their movement along chemical gradients. In contrast to swimming, however, we find that the swimming chemotaxis cluster (Che cluster I) is not required for chemotaxis on surfaces because CheY1 mutants perform twitching chemotaxis (*SI Appendix*, Fig. S6).

Recent work has shown that twitching motility in *P. aeruginosa* is under the regulation of a separate signal-transduction pathway (Che cluster IV) known as the Chp system (16, 29) (Fig. 3*B*), but to date, there is no direct evidence that this system plays an active role in any form of chemotaxis. To examine the effects of the Chp system, we first recapitulated the motility phenotypes recently described using classical agar-based assays (29). Specifically, in-frame deletion mutants Δ*pilB,* Δ*chpA*, and Δ*pilG* do not form the characteristic twitching rings at the plastic–agar interface around colonies, whereas Δ*pilH* cells exhibit an intermediate phenotype by producing rings that are smaller than that of the WT (*SI Appendix*, Fig. S7). However, observing the movement of individual cells in our microfluidic system reveals a very different pattern. We find that Δ*chpA* and Δ*pilG* cells, which were previously diagnosed as incapable of twitching (29), are in fact both motile (Fig. 3 *A* and *C*). While Δ*pilH* cells show reduced twitching rings on agar plates (*SI Appendix*, Fig. S7), in our microfluidic assays they actually move ≈30 times faster than the WT (Fig. 3 *A* and *C*) and tend to orient themselves vertically on the surface (*SI Appendix*, Fig. S8). More formally, the root mean squared displacement (RMSD), a combined measure of both movement speed and the persistence in movement direction (30), of the WT and Δ*pilG* cells are nearly identical, but show strong differences with that from Δ*chpA* and Δ*pilH* (Fig. 3*C*).

The Chp system then has strong effects on twitching motility in our assay but is it involved in chemotaxis? To answer this question, we focused on the response regulator of the Chp system PilG, which controls pili extension (29). We focused on PilG because the motility of Δ*pilG* is similar to the WT in our microfluidic assay, and we can study the effects on chemotaxis in the absence of strong effects on motility (Fig. 3 *A* and *C* and Movies S3 and S4). We exposed Δ*pilG* cells to a stable DMSO gradient and used our analysis pipeline to track individual cells. The data reveal that, although Δ*pilG* cells indeed remain motile, they lack the ability to bias their motion up the gradient (Fig. 3 *D* and *E*). Our results then suggest that the Chp system is not just involved in the biosynthesis of type IV pili but also in the transduction of chemotactic stimuli into directed movement.

***P. aeruginosa* Uses a "Pessimistic" Chemotactic Strategy on Surfaces.** We next sought to understand how *P. aeruginosa* cells bias their movement on surfaces. Chemotaxis in swimming *E. coli* cells is achieved by cells performing straight runs interspersed by sharp reorientations (tumbles), where tumbles are delayed when moving up a chemoattractant gradient (2, 3). Do twitching bacteria use similar movement strategies in our experiments? Although twitching motility gets its name from the jerky motion that cells exhibit over the timescale of minutes (31), we find that in chemical gradients cells can maintain a consistent movement direction for periods longer than 1 h (Fig. 4*A*). Moreover, these twitching runs are interspersed by events where a cell reverses by stopping and then moving back in the opposite direction without turning. Twitching *P. aeruginosa* cells pull themselves along surfaces with pili that cluster at their poles (32, 33), which drives movement parallel to their long axis (*SI Appendix*, Fig. S9) and allows rapid changes in direction if a cell changes the pole that it is pulling from. To follow this process, we developed an automated algorithm that detects when the cell's movement switches direction such that a cell's leading pole becomes its trailing pole. Importantly, we distinguish these active reversals from changes in direction that occur passively due to cell division (Fig. 4 *A* and *B*, Movies S3 and S4, and *SI Appendix, SI Materials and Methods*).

Both Δ*pilG* and WT cells were found to actively reverse their direction in both the presence and absence of DMSO gradients. However, Δ*pilG* cells, which do not show chemotaxis (Fig. 3 *D* and *E*), reversed at a much lower rate than WT cells in both of these conditions, suggesting that the reversals are indeed important for chemotaxis (Fig. 4*C*). To examine the potential link

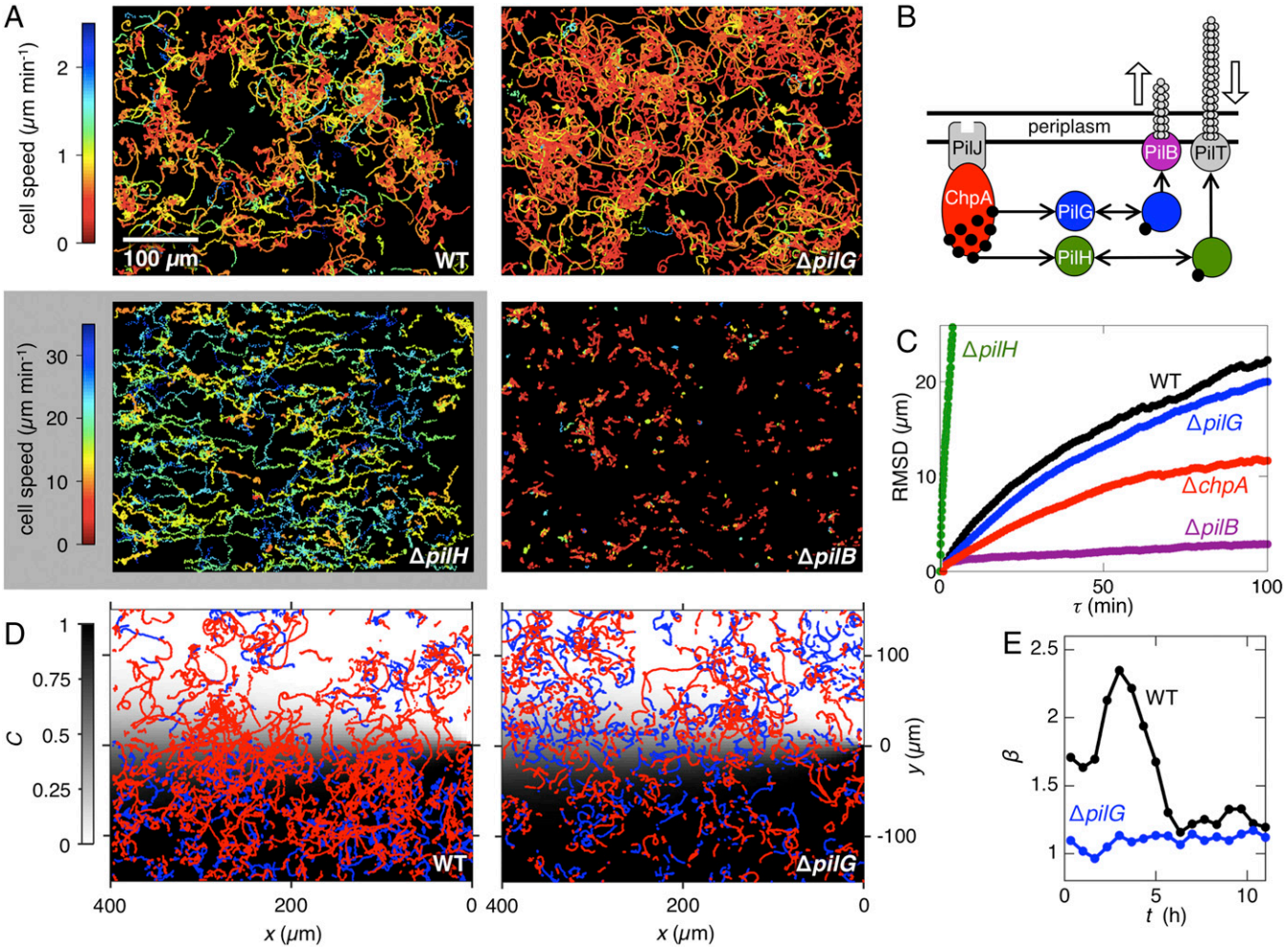

Fig. 3. Twitching chemotaxis in *P. aeruginosa* is mediated by the Chp signal transduction pathway. (*A*) Trajectories of WT and different Chp mutants in the absence of a chemical gradient where color denotes instantaneous cell speed. (*B*) Simplified diagram of Chp chemosensory system. By homology to the Che system of *E. coli*, it is thought that the protein kinase ChpA drives phosphorylation of two CheY-like response regulator proteins, PilG and PilH. These response regulators interact with the ATPases PilB and PilT to drive pilus extension and retraction, respectively, in a manner similar to how phosphorylated CheY controls flagellar rotation in swimming cells (29). Black circles denote phosphate groups. (*C*) *RMSD* of different strains in the absence of a chemical gradient as a function of time lag, τ. Analysis of a large number of cells (*SI Appendix*, Fig. S16*A*) reveals Δ*pilG* cells move similarly to the WT, Δ*pilH* cells move much faster (note separate color bar in *A*), Δ*chpA* cells move at an attenuated rate, and Δ*pilB* cells lack motility altogether (also see *SI Appendix*, Fig. S16*B*). (*D*) Trajectories of Δ*pilG* and its respective WT in a DMSO gradient reveals that PilG plays an essential role in twitching chemotaxis. Here trajectories with net movement toward larger *C* are shown in red and those with net movement toward smaller *C* are shown in blue. (*E*) These findings are confirmed by measurements of the chemotactic bias, β, which show quantitatively that Δ*pilG* cells lack the ability to perform chemotaxis. Data used to compose *A* and *C* for Δ*pilH* cells were collected in the first 15 min after inoculation as they move so quickly, whereas data from the remainder of strains in these panels was collected over the first 10 h. *D* shows trajectories over the first 8 h of the experiment, when chemotaxis is most pronounced (*E*).

between reversal rate and the ability to perform chemotaxis, we analyzed how the reversal rate changes as a function of the direction that cells are moving. This analysis revealed that Δ*pilG* cells reverse at nearly the same rate whether they are moving toward or away from the chemoattractant (Fig. 4*C*). In sharp contrast, WT cells almost double their reversal rate when moving away from the source of a chemoattractant but keep their basal reversal rate when moving toward the source (Fig. 4*C*). This observation is consistent with a "pessimistic" chemotactic strategy where cells respond to a reduction in the chemoattractant concentration (23), which contrasts with the "optimistic" strategy used by swimming *E. coli* that chemotax by postponing tumbles when moving toward a chemoattractant source (2, 3). Put another way, swimming *E. coli* respond "if life gets better" (2) and our data show that twitching *P. aeruginosa* respond if life gets worse. We also find asymmetries in speed: WT cells move ≈25% faster when traveling toward the source compared with away from it (*SI Appendix*, Fig. S10). In contrast, Δ*pilG* cells moving toward and away from the chemoattractant source travel at approximately the same rate (*SI Appendix*, Fig. S10). Taken together, our data suggest that the response regulator PilG enables the movement of surface-attached bacteria up chemical gradients by modulating both reversal rate and cell speed.

Surface-Attached Bacteria Can Control Their Movements with Submicron Precision. Swimming *P. aeruginosa* cells navigate chemical gradients by selectively rotating their flagella in the opposite direction, which sharply changes their direction of movement (5). In contrast, we show that surface-attached bacteria can climb chemical gradients by regulating when they switch directions by pulling themselves using pili attached to the previously trailing pole. Our observations suggest that this system is extremely effective at guiding attached cells toward larger concentrations of chemoattractants (Movie S2). However, just how responsive are individual attached cells to changes in their chemical environment? To probe the limits of the cells' abilities, we designed and built a microfluidic device that allows us to continuously track cells as they respond to a DMSO gradient

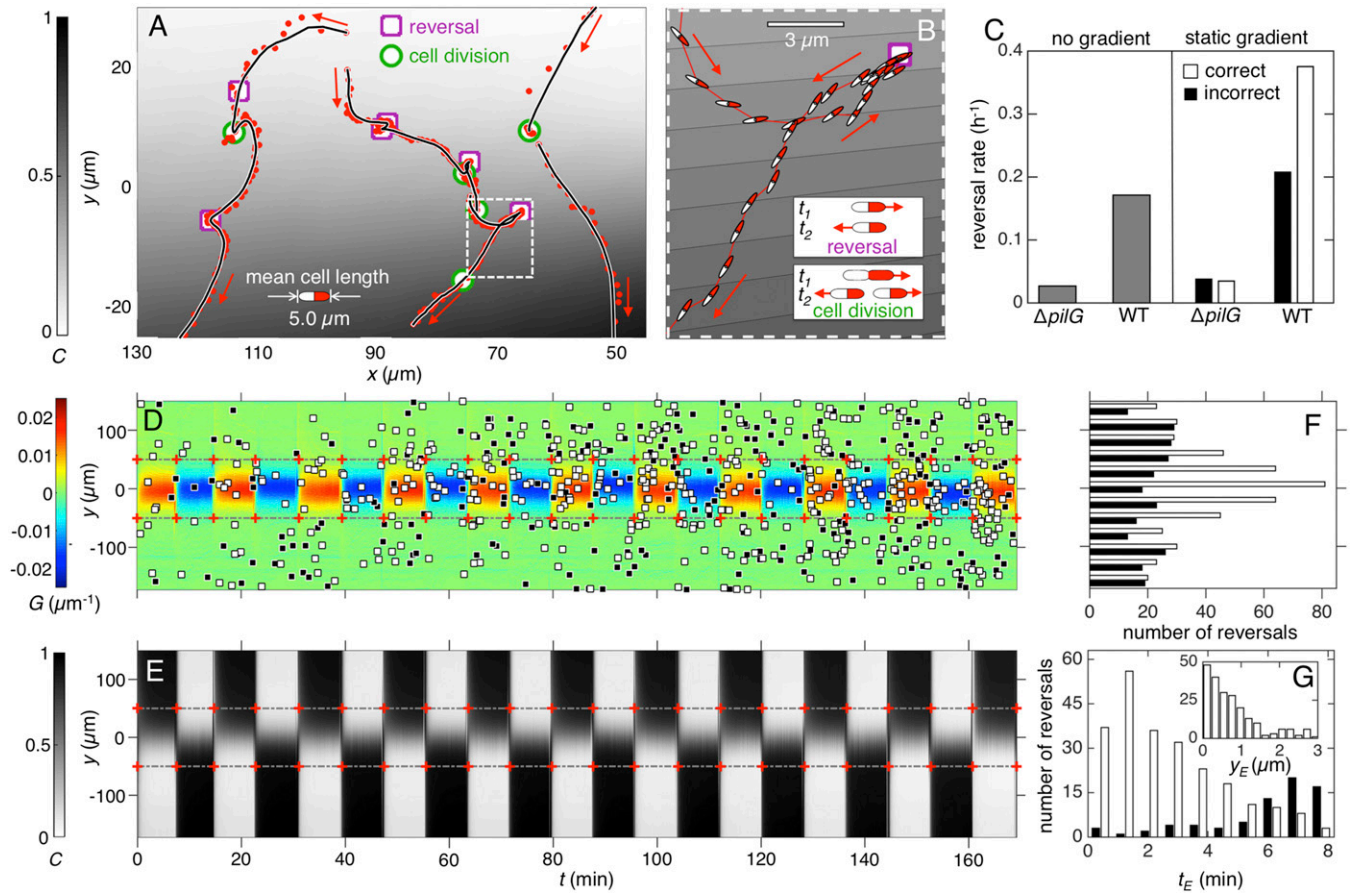

Fig. 4. Twitching bacteria chemotax by reversing their motility when traveling away from the chemoattractant source. (*A*) Cells navigate up DMSO gradients by actively performing reversals (magenta squares), although sharp changes in direction can also occur passively during cell division (green circles). Red dots in *A* show positions of cell centroids at 1-min intervals; the black lines show smoothed trajectories, and the average cell length is shown for reference. (*B*) Magnified view of a reversal shows a cell whose movement begins to veer toward decreasing *C*. The cell quickly performs a reversal sending it back up the DMSO gradient. Ellipses (not drawn to scale) show cell orientation and position in 2-min intervals. Contours show modeled DMSO concentration in $C_{MAX}/30$ increments where $C_{MAX} = 350$ mM. (*C*) In both the absence and presence of a DMSO gradient Δ*pilG* cells actively reverse at a much smaller rate than WT cells. For experiments with a DMSO gradient, we calculated the frequency that cells moving toward smaller *C* reverse direction (labeled correct, white bars) and the frequency that cells moving toward larger *C* reverse direction (labeled incorrect, black bars). Although the rate of incorrect reversals in the WT is similar to that in the absence of a gradient (gray bar), correct reversals occur more frequently, suggesting that reversals are deployed as a corrective strategy. (*D*–*G*) Using a custom microfluidic device (*SI Appendix*, Fig. S11), we induced reversals by exposing cells to a DMSO gradient that changed direction every eight minutes. Owing to a large flow velocity, *C* and its gradient $G = 1/C_{MAX}\,\partial C/\partial y$ were nearly constant along our field of view, allowing us to average them along *x* and present their spatiotemporal variations using kymographs (*D* and *E*) (*SI Appendix, SI Materials and Methods*). Cell reversals were identified using an automated algorithm and classified as correct (white squares, *D*) or incorrect (black squares, *D*). Both types of reversals increased over time as cell division and attachment increased the number of cells on the surface (*D*). Counting the number of correct and incorrect reversals within equally spaced bins in *y* reveals that correct reversals (white bars, *F*) peak along the middle of the device, whereas the number of incorrect reversals (black bars, *F*) occurs more uniformly in *y*. The reaction time, t_E, is the time elapsed from the most recent gradient change (red + symbols in *E* and *F*) to the time of a correct reversal. A histogram of t_E for cells in middle 100 μm of the device (dashed gray lines; *D* and *E*) shows that correct reversals peak ≈1 min after the gradient changes direction (*G*). Over this period most cells travel a distance along the gradient, y_E, less than 1 μm (*G*, *Inset*).

that changes direction every eight minutes (Fig. 4 *D* and *E* and *SI Appendix*, Fig. S11). Direct observation suggests that twitching *P. aeruginosa* cells accurately reverse their movement in response to the alternating gradient (Movie S5), and we quantified their response by categorizing all reversal events as correct or incorrect. Correct reversals occurred in cells moving away from the chemoattractant source and incorrect reversals occurred in cells moving toward the source (Fig. 4 *D* and *E* and Movie S6). We find that correct reversals are stimulated by the alternating gradient (rather than incorrect reversals being repressed), which is again consistent with a pessimistic chemotactic response (Fig. 4*F*). In addition, we find that WT cells actively increase their speed after performing correct reversals but not after performing incorrect reversals (*SI Appendix*, Fig. S12). In contrast, cells lacking PilG reversed very rarely in the alternating chemical gradient (*SI Appendix*, Fig. S13). Taken together, these observations show that attached *P. aeruginosa* chemotax by deploying reversals when their motility is directed away from the source of a chemoattractant. Correct reversals occurred most frequently in the middle of the device, where cells are exposed to the strongest spatial gradients in DMSO (Fig. 4 *D* and *F*) and these reversals peak $t_E \approx 1$ min after the gradient changes direction (Fig. 4*G*). The rapid response means that the majority of cells sense the gradient has changed direction and respond before moving one-fifth the length of their bodies (*SI Appendix*, Fig. S14), a distance smaller than a micrometer (Fig. 4*G*, *Inset*). This observation reveals that attached *P. aeruginosa* can regulate their movement in a chemical gradient with submicron precision.

Swimming bacteria sense chemoattractant gradients by measuring changes in chemical concentrations over time, which is consistent with them moving rapidly and thus being able to detect large changes over short time periods (2, 34). However, the slow speed and highly unsteady, oscillatory movement of twitching cells (31) begs the

question of whether they too use temporal sensing. If twitching cells do use temporal sensing, it would require the integration of information over much longer time-scales than swimming bacteria. Moreover, a twitching cell would have to extract the slow, weak changes in concentration due to their average movement from the large, high-frequency changes in concentration that arise from a cell jerking back and forth relative to a chemical gradient. An intriguing alternative is that twitching cells detect gradients spatially by directly measuring changes in concentration across the length of their bodies. Indeed, in our experiments (Fig. 4 *D*–*G*), the majority of responding cells experience a fivefold larger change in chemoattractant concentration across their length than they experience over time due to their movement relative to the gradient (*SI Appendix*, Fig. S14). Although the fast movement of swimming cells allow them to measure changes in concentration over distances equivalent to tens of their body lengths (2), the slow movement of twitching cells suggests that they could collect more reliable information by making spatial measurements, over the length of their body. In either case, our data suggest that the molecular mechanisms underlying twitching chemotaxis have very different properties than the canonical mechanisms so intensively studied in swimming cells.

Conclusion

Bacteria often live attached to surfaces where multiple strains and species meet and interact (35). These cells strongly alter their environment by secreting a wide range of compounds and metabolizing others to create a diverse and changing set of chemical gradients (8). The resulting chemical gradients can be very steep, stable, and important for the fitness of cells that lie in different positions within a community (36). Here we showed that single attached bacteria can respond to chemical gradients. Rather like ants moving through a nest, we find that twitching cells are able to act as individuals that navigate their way through their chemical and biological environment. We also show that these surface-attached cells perform chemotaxis on spatial scales much finer than swimming cells, with corrective maneuvers occurring before a cell has moved a small fraction of their body length. The discovery that bacteria can navigate their chemical environment with submicron precision has implications for both the biology of bacterial communities and how we manipulate them.

Materials and Methods

Our experiments use WT *P. aeruginosa* PAO1 (Kolter collection, ZK2019) as a working model for twitching chemotaxis (Figs. 1 and 2 and *SI Appendix*, Figs. S3, S9, and S15). The YFP-labeled strain used in Fig. 1 *F* and *G* and *SI Appendix*, Fig. S1 is a PAO1 WT strain with a ZK2019 background (37). Δ*flgK* (*SI Appendix*, Fig. S5), which has been published and described before (38), is a deletion strain lacking the hook filament junction protein FlgK. To study the functional role of the Chp chemosensory system, we used in-frame deletion mutants of *pilB*, *chpA*, *pilG*, and *pilH*, along their respective WT, which have all been published and described elsewhere (29). These strains are used in Figs. 3 and 4 and *SI Appendix*, Figs. S4, S7, S8, S10, S12–S14, and S16. The Δ*cheY*1 mutant strain shown in *SI Appendix*, Fig. S6 was a gift from the group of Caroline Harwood, University of Washington, Seattle. All strains were grown in shaken culture overnight in LB (37 °C) from frozen stocks and subcultured to obtain cells in exponential phase. These were then diluted to an optical density of 0.25 (at 600 nm) in tryptone broth (TB; 10 g Bacto tryptone/1 L water) before they were injected into our microfluidic devices.

ACKNOWLEDGMENTS. We thank Joanne Engel for the Pil-Chp mutants, Caroline Harwood for the CheY1 mutant, Jean-Yves Tinevez for help with the Trackmate code, and Michael Laub for discussions. Judith Armitage, Howard Berg, Eamonn Gaffney, Jeffery Guasto, Michael Laub, Timothy Pedley, Roman Stocker, and Gerard Wong provided comments on preliminary versions of this manuscript. This work was funded by a Fundação para a Ciência e Tecnologia Studentship SFRH-BD-73470-2010 (to N.M.O.), European Research Council Grant 242670 (to K.R.F.), and a Human Frontier Science Program Fellowship LT001181/2011L (to W.M.D.).

1. Adler J (1966) Chemotaxis in bacteria. *Science* 153(3737):708–716.
2. Berg HC (2004) *E. coli in Motion* (Springer, New York).
3. Berg HC, Brown DA (1972) Chemotaxis in *Escherichia coli* analysed by three-dimensional tracking. *Nature* 239(5374):500–504.
4. Wadhams GH, Armitage JP (2004) Making sense of it all: Bacterial chemotaxis. *Nat Rev Mol Cell Biol* 5(12):1024–1037.
5. Porter SL, Wadhams GH, Armitage JP (2011) Signal processing in complex chemotaxis pathways. *Nat Rev Microbiol* 9(3):153–165.
6. Costerton JW, Lewandowski Z, Caldwell DE, Korber DR, Lappin-Scott HM (1995) Microbial biofilms. *Annu Rev Microbiol* 49:711–745.
7. Kolter R, Greenberg EP (2006) Microbial sciences: The superficial life of microbes. *Nature* 441(7091):300–302.
8. Stewart PS, Franklin MJ (2008) Physiological heterogeneity in biofilms. *Nat Rev Microbiol* 6(3):199–210.
9. Klausen M, Aaes-Jørgensen A, Molin S, Tolker-Nielsen T (2003) Involvement of bacterial migration in the development of complex multicellular structures in *Pseudomonas aeruginosa* biofilms. *Mol Microbiol* 50(1):61–68.
10. Klausen M, et al. (2003) Biofilm formation by *Pseudomonas aeruginosa* wild type, flagella and type IV pili mutants. *Mol Microbiol* 48(6):1511–1524.
11. Zhao K, et al. (2013) Psl trails guide exploration and microcolony formation in *Pseudomonas aeruginosa* biofilms. *Nature* 497(7449):388–391.
12. Shi W, Köhler T, Zusman DR (1993) Chemotaxis plays a role in the social behaviour of *Myxococcus xanthus*. *Mol Microbiol* 9(3):601–611.
13. Zhang Y, Ducret A, Shaevitz J, Mignot T (2012) From individual cell motility to collective behaviors: Insights from a prokaryote, *Myxococcus xanthus*. *FEMS Microbiol Rev* 36(1):149–164.
14. Kearns DB, Robinson J, Shimkets LJ (2001) *Pseudomonas aeruginosa* exhibits directed twitching motility up phosphatidylethanolamine gradients. *J Bacteriol* 183(2):763–767.
15. Miller RM, et al. (2008) *Pseudomonas aeruginosa* twitching motility-mediated chemotaxis towards phospholipids and fatty acids: Specificity and metabolic requirements. *J Bacteriol* 190(11):4038–4049.
16. Sampedro I, Parales RE, Krell T, Hill JE (2015) *Pseudomonas* chemotaxis. *FEMS Microbiol Rev* 39(1):17–46.
17. Taylor RG, Welch RD (2008) Chemotaxis as an emergent property of a swarm. *J Bacteriol* 190(20):6811–6816.
18. O'Toole GA, Kolter R (1998) Flagellar and twitching motility are necessary for *Pseudomonas aeruginosa* biofilm development. *Mol Microbiol* 30(2):295–304.
19. Burrows LL (2012) *Pseudomonas aeruginosa* twitching motility: Type IV pili in action. *Annu Rev Microbiol* 66(66):493–520.
20. Adler J, Hazelbauer GL, Dahl MM (1973) Chemotaxis toward sugars in *Escherichia coli*. *J Bacteriol* 115(3):824–847.
21. Shi W, Köhler T, Zusman DR (1994) Isolation and phenotypic characterization of *Myxococcus xanthus* mutants which are defective in sensing negative stimuli. *J Bacteriol* 176(3):696–701.
22. Seymour JR, Simó R, Ahmed T, Stocker R (2010) Chemoattraction to dimethylsulfoniopropionate throughout the marine microbial food web. *Science* 329(5989):342–345.
23. Packer HL, Gauden DE, Armitage JP (1996) The behavioural response of anaerobic *Rhodobacter sphaeroides* to temporal stimuli. *Microbiology* 142(Pt 3):593–599.
24. Kaiser D (2003) Coupling cell movement to multicellular development in myxobacteria. *Nat Rev Microbiol* 1(1):45–54.
25. Moulton RC, Montie TC (1979) Chemotaxis by *Pseudomonas aeruginosa*. *J Bacteriol* 137(1):274–280.
26. Rivero MA, Tranquillo RT, Buettner HM, Lauffenburger DA (1989) Transport models for chemotactic cell populations based on individual cell behavior. *Chem Eng Sci* 44(12):2881–2897.
27. Conrad JC, et al. (2011) Flagella and pili-mediated near-surface single-cell motility mechanisms in *P. aeruginosa*. *Biophys J* 100(7):1608–1616.
28. Kato J, Kim HE, Takiguchi N, Kuroda A, Ohtake H (2008) *Pseudomonas aeruginosa* as a model microorganism for investigation of chemotactic behaviors in ecosystem. *J Biosci Bioeng* 106(1):1–7.
29. Bertrand JJ, West JT, Engel JN (2010) Genetic analysis of the regulation of type IV pilus function by the Chp chemosensory system of *Pseudomonas aeruginosa*. *J Bacteriol* 192(4):994–1010.
30. Gibiansky ML, et al. (2010) Bacteria use type IV pili to walk upright and detach from surfaces. *Science* 330(6001):197.
31. Jin F, Conrad JC, Gibiansky ML, Wong GCL (2011) Bacteria use type-IV pili to slingshot on surfaces. *Proc Natl Acad Sci USA* 108(31):12617–12622.
32. Cowles KN, Gitai Z (2010) Surface association and the MreB cytoskeleton regulate pilus production, localization and function in *Pseudomonas aeruginosa*. *Mol Microbiol* 76(6):1411–1426.
33. Skerker JM, Berg HC (2001) Direct observation of extension and retraction of type IV pili. *Proc Natl Acad Sci USA* 98(12):6901–6904.
34. Segall JE, Block SM, Berg HC (1986) Temporal comparisons in bacterial chemotaxis. *Proc Natl Acad Sci USA* 83(23):8987–8991.
35. Nadell CD, Xavier JB, Foster KR (2009) The sociobiology of biofilms. *FEMS Microbiol Rev* 33(1):206–224.
36. Kim W, Racimo F, Schluter J, Levy SB, Foster KR (2014) Importance of positioning for microbial evolution. *Proc Natl Acad Sci USA* 111(16):E1639–E1647.
37. Oliveira NM, et al. (2015) Biofilm formation as a response to ecological competition. *PLoS Biol* 13(7):e1002191.
38. Caldara M, et al. (2012) Mucin biopolymers prevent bacterial aggregation by retaining cells in the free-swimming state. *Curr Biol* 22(24):2325–2330.
39. Shen Y, Siryaporn A, Lecuyer S, Gitai Z, Stone HA (2012) Flow directs surface-attached bacteria to twitch upstream. *Biophys J* 103(1):146–151.